Progress In Electromagnetics Research, Vol. 138, 157–171, 2013

FEATURE EXTRACTION FOR LANDMINE DETECTION IN UWB SAR VIA SWD AND ISOMAP

Jun Lou*, Tian Jin, and Zhimin Zhou

School of Electronic Science and Engineering, National University of Defense Technology (NUDT), Changsha, Hunan 410073, China

Abstract—Ultra-wideband synthetic aperture radar (UWB SAR) is a sufficient approach to detect landmines over large areas from a safe standoff distance. Feature extraction is the key step of landmine detection processing. On the one hand, the feature vector should contain more scattering characteristics to discriminate landmines from clutters; on the other hand, the dimensionality of feature vector should be lower to avoid the "curse of dimensionality". In this paper, a novel feature vector extraction method is proposed. We first obtain the scattering characteristics in four domains, i.e., range, azimuth, frequency and aspect-angle, via the space-wavenumber distribution (SWD). Since the data after SWD are with higher dimension and local nonlinear structures, a typical manifold learning method, Isomap, is used to reduce the dimension. The validity of the proposed method is proved by using the real data collected by an airship-borne UWB SAR system.

1. INTRODUCTION

Ultra-Wide Band Synthetic Aperture Radar (UWB SAR) with the ground penetrating capability has become an alternative way to detect landmines over large areas [1–3]. The typical detection procedure is first to extract the Regions of Interest (ROIs) from the entire SAR image, which is called prescreening in this paper. Each ROI contains a mine-like target. Some mine-like targets are landmines, whereas some are only clutters. In prescreening, high detection probability is desired, which leads to a high false alarm rate. The next step is to detect landmines from clutters in the extracted ROIs, which is called detection processing here. Detection should reject clutters

Received 13 December 2012, Accepted 15 March 2013, Scheduled 18 March 2013

* Corresponding author: Jun Lou (loujun@nudt.edu.cn).

as many as possible while maintaining a high detection probability. Detection processing includes two main steps: feature extraction and detector design. Features are obtained through the feature extraction procedure and then formed the feature vector for the following detector. Numerous studies have focused on the detector design, such as k-Nearest Neighbors (KNN), Support Vector Machine (SVM) [4–6] and Neural Network [7, 8]. However, a set of suitable features may achieve a correct detection, even if using a simple detector; on the contrary, it could be difficult to achieve a satisfactory detection performance without well-selected features of landmines, even if using a complex detector. Therefore, we focus on feature extraction in this paper.

The ROI image data generated by SAR system usually has very high dimension and very limited number of samples. The target detection based on it is a typical high-dimensional identification of small samples, which is one of the most difficult problems in the modern pattern classification study. In UWB SAR, a metallic antitank landmine often yields two dominant scattering centers along the range direction, which correspond to the front and rear edges of the top surface of the landmine and is called double-hump signature [9, 10]. Therefore, the range cut through the ROI image center is usually used as the input feature vector for landmine detection, which has the two-peak characteristic [11]. This feature has lower dimension than the whole ROI image and is suitable to discriminate the clutter without two peaks, which will reduce the false alarm rate. However, this method still cannot fulfill the practical requirement, due to that the range cut data only use the scattering characteristic in range domain. Frequency features are another consideration due to the wide bandwidth of radar. For example, the features of sub-bands with good target-to-clutter contrast are input into a classifier designed based on Fischer's linear discriminant in [12]. The time-frequency (TF) analysis can extract the target features of the time domain and the frequency domain simultaneously, which yields a potentially more revealing image of the ROI range components [13–15]. However, these studies do not provide much attention to the azimuth characteristics of target scatterings. Actually, the scattering characteristics of landmine represent at least in the four domains: range, azimuth, frequency and aspect-angle, which can be obtained by the space-wavenumber distribution (SWD) method. However, it means that we need to process the data with higher dimension if we want to use more characteristics.

To solve this problem, we need to reduce the dimension without losing information. Principal Component Analysis (PCA) [16–18] and Linear Discriminant Analysis (LDA) [19] are two typical linear dimension reduction methods. Linear methods suppose that the

data are global linear and attempt to maintain consistent Euclidean distances between points in the low-dimensional embeddings. However, the UWB SAR imaging is interfered by many factors, such as radio frequency interference [20], motion of the platform [21], and speckle [22]. These complexities of SAR imaging results in the existence of local nonlinear structures, the linear dimension reduction approaches are no longer appropriate for landmine detection in UWB SAR. Manifold learning is a newly proposed machine learning theory, which is a nonlinear dimension reduction method [23, 24]. Nonlinear techniques attempt to maintain consistent geodesic distances (distances along the manifold) in the low-dimensional embedding. In this paper, we propose a novel landmine detection method based on the manifold learning. The proposed method firstly uses the SWD processing to obtain images with different frequencies and aspect-angles of an original ROI image, which exhibits the scattering characteristics of the target. Then we use a typical manifold learning method which is called Isomap to obtain low-dimensional feature vector for detection.

The remainder of the paper is organized as follows. Section 2 introduces the traditional feature extraction methods for landmine detection. Section 3 proposes our feature extraction method. Section 4 proves the validity of the proposed method by using real data collected by an airship-borne UWB SAR system. Section 5 provides the conclusion.

2. TRADITIONAL FEATURE EXTRACTION METHODS FOR LANDMINE DETECTION

The dimensionality will be very high if we form the feature vector pixel by pixel from the original ROI image. Such high dimension will encounter the "curse of dimensionality": the amount of data needed for robust statistical modeling grows exponentially in the dimensionality. It means that we need a huge number of samples of landmines, which are hard to be obtained in practice. To solve this problem, we need to form the feature vector with low-dimensionality. Traditionally, there are two ways to extract features from an image: extraction of features defined by domain experts and data-driven subspace projection. The former way is based on the experience and computationally tractable. For landmine detection in UWB SAR image, 1D range cut through the ROI image center is taken as the feature vector by experience. The latter way is based on data analysis, the PCA is used to find the subspace projection and form the feature vector for landmine detection.

2.1. Taking 1D Range Cut as Feature Vector

Figure 1(b) shows a SAR image of a metallic landmine (Fig. 1(a)) with the diameter of 0.3 m, which is obtained by an Airship-Mounted UWB SAR (AMUSAR) system with the operating frequency band of 0.5–2.5 GHz and the accumulated angle of 60° [25]. There are two salient scattering centers along the range direction, which can be called the double-hump. The double-hump corresponds to the strong scattering

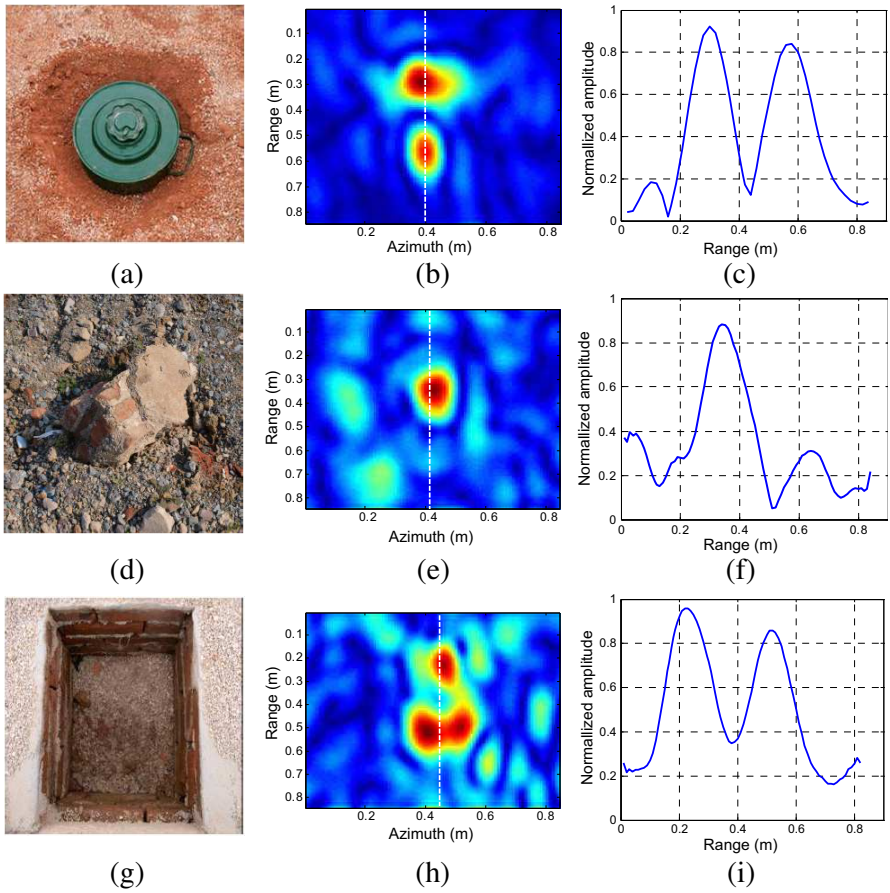

Figure 1. (a) Optical image of a metallic landmine; (b) SAR image of a metallic landmine; (c) 1D range cut of landmine; (d) Optical image of a clutter; (e) SAR image of a clutter; (f) 1D range cut of a clutter; (g) Optical image of a hole; (h) SAR image of a hole; (i) 1D range cut of hole.

echo from the front and rear edges of the landmine. Since the shape of most clutters are different from landmine, most clutters do not have the double-hump as shown in Figs. 1(d) and 1(e). Therefore, the double-hump is an important characteristic to distinguish landmines from clutters. 1D range cut through the image center as shown in the Fig. 1(c) can well exhibit the double-hump characteristic, and the dimensionality of 1D range cut is much lower than the original image, so people usually take 1D range cut as the feature vector. However, 1D range cut only represents the scattering characteristics in range direction. Some clutters may also have double-hump in the 1D range cut. For example, a clutter shown in Fig. 1(g) also exhibits double-hump in the 1D range cut as shown in Fig. 1(i). Practically, this clutter can be distinguished via the characteristics in the azimuth direction, which is discarded in the 1D range cut. As a result, taking 1D range cut as the feature vector is defective.

2.2. Using PCA to Form Feature Vector

In order to form a low-dimensional feature vector without losing characteristics of image, some people use data-driven subspace projection method to find the projection from the original high-dimensional image space to a lower-dimensional subspace. A classical data analysis method, principal component analysis (PCA), is usually used to form the feature vector for landmine detection.

PCA assumes that data can be characterized with coordinates in linear subspaces with lower dimensionality. The coordinates can be computed as a linear projection from the original high-dimensional space such that they can be used to optimally reconstruct the original data points. PCA is especially computationally tractable and scales to both large-scale and very high-dimensional data sets. The core step is to diagonalize the covariance matrix of the data. Alternatively, one can diagonalize the Gram matrix, with elements being the pairwise inner products between data points. However, despite its popularity and wide application, PCA is inadequate in capturing interesting structures in data if the data do not live in a linear subspace. The UWB SAR imaging is interfered by many factors, such as radio frequency interference, motion of the platform, and speckle. These complexities of SAR imaging result in the existence of local nonlinear structures. Under these circumstances, PCA as a linear dimension reduction approach is helpless.

3. PROPOSED FEATURE EXTRACTION METHOD

From above analysis, we can find that the key of feature extraction for landmine detection is to form a lower-dimensional feature vector with more scattering characteristics of the target from the SAR image. In this section we proposed a novel feature extraction method which is composed of two parts, i.e., the space-wavenumber distribution processing and the Isomap dimension reduction method. The former part is used to obtain scattering characteristics in four domains, i.e., range, azimuth, frequency and aspect-angle; and the latter part is used to form a lower-dimensional feature vector.

3.1. Space-wavenumber Distribution Processing

Because of the differences in the principles of imaging, SAR image is quit different from optical image. Taking the strip map SAR for example, since the SAR image is synthesized by the data from the antenna at different positions along the flight path as shown in Fig. 2, the SAR image contains the aspect-angle characteristics of the target, whereas the optical image does not. Besides, the response of the target with different frequency is different, which can be used in detection. The UWB SAR has a large bandwidth, so the SAR image also contains abundant frequency characteristics of the target.

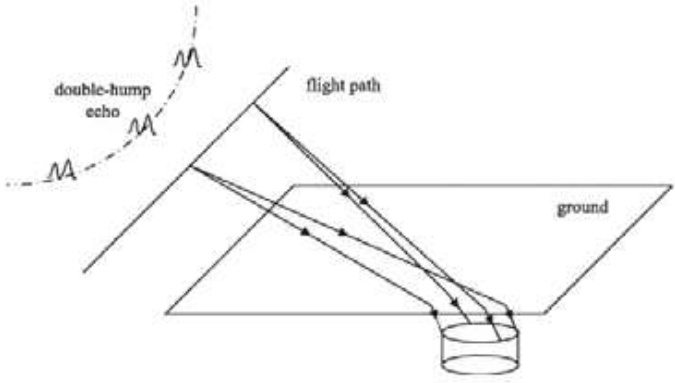

Figure 2. Strip-map SAR imaging geometry.

From the above analysis, the UWB SAR image contains 4-D target scattering information of range, azimuth, frequency, and aspect-angle. For a landmine, the scattering characteristics represent in these four domain: in the range direction, a metallic landmine often

yields two dominant scatterers corresponding to the front and rear edges of the top of the landmine; in the azimuth direction, there is at most only one scattering center; in the frequency domain, UWB SAR system commonly operate in low frequency band (< 3 GHz) which can be defined as resonance band for a landmine, thus the response of the landmine in the frequency domain is respected to the shape and size of the landmine [26]; in the aspect-angle domain, a landmine can be regarded as a body of revolution (BOR) with its axis rotating perpendicular to the ground, thus the scattering caused by the landmine is invariable to the various aspect-angles.

However, these characteristics are embedded in the raw data, but these data are not always available directly, so it will be

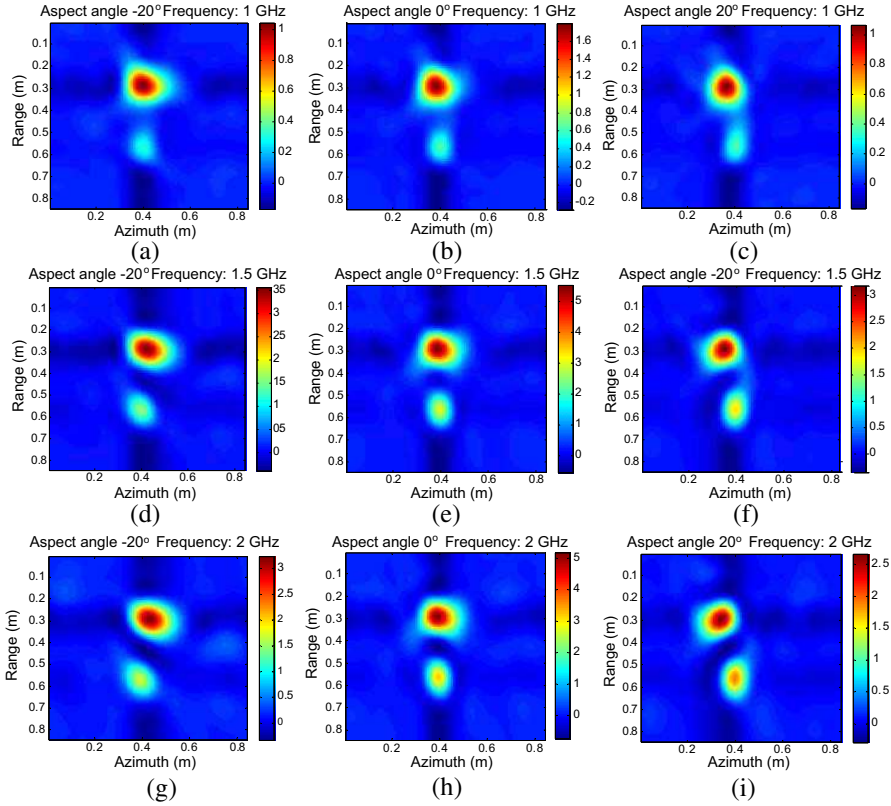

Figure 3. CWD-based SWD processing result of the ROI image in Fig.1(b): (a) 1 GHz, $-20°$; (b) 1 GHz, $0°$; (c) 1 GHz, $20°$; (d) 1.5 GHz, $-20°$; (e) 1.5 GHz, $0°$; (f) 1.5 GHz, $20°$; (g) 2 GHz, $-20°$; (h) 2 GHz, $0°$; (i) 2 GHz, $20°$.

beneficial to retrieve these variations from the synthesized data. Several people proposed Subband-Subaperture method to acquire SAR images of same scene with different frequency bands and aspect-angle bounds, but it brought a sacrifice of the range and azimuth resolution [27]. In [28], we proposed a SWD method based on the idea of Time-Frequency Analysis (TFA), and identified that the Subband-Subaperture method which actually relied on Short-Time Fourier Transform (STFT) was a member of SWD. In addition, [28] developed a SWD method based on the theory of Choi-Williams distribution, which overcomes the STFT in terms of spatial resolutions.

For instance, The CWD-based SWD processing result of this ROI image is shown in the Fig. 3. Nine images are obtained with three different frequencies (1 GHz, 1.5 GHz and 2 GHz) and three different aspect-angles ($-20°$, $0°$ and $20°$), which represent the landmine scattering characteristics in four domains: range, azimuth, frequency, and aspect-angle.

3.2. Dimension Reduction

We have obtained images with different frequencies and aspect-angles of an original ROI image. These images exhibit the scattering characteristics, but are not suitable to form the feature vector pixel by pixel directly because the image data have very high dimensionality. Since the SAR image data always lie on a complex nonlinear manifold, nonlinear dimension reduction technique is more reasonable than linear dimension reduction to discover the intrinsic structure in the data. Manifold learning is a newly proposed nonlinear dimension reduction method recent years. It focuses on finding the inherent distribution of the high dimension datasets and solving the corresponding projections.

For example, Fig. 4(a) shows three points A, B, and C on a polarimetric manifold, on which the same color represents the

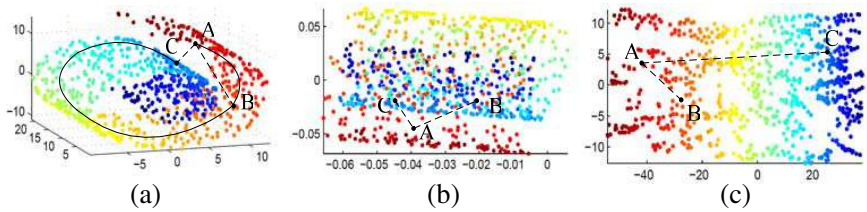

Figure 4. Illustrative example of PCA and nonlinear method: (a) Original polarimetric manifold in 3-D space; (b) Two-dimensional embedding by PCA; (c) Two-dimensional embedding by nonlinear method.

same class. The dashed line represents Euclidean distance between two points, and the solid line represents geodesic distance which is measured along the polarimetric manifold surface. In Fig. 4(a), points A and B belong to the same class, whereas point C belongs to another. However, point A is closer to point C compared to point B under the Euclidean distance, which may lead to the misclassification those points A and C belong to the same class, whereas point B belongs to another. In Fig. 4(c), the polarimetric manifold is mapped into a low-dimensional intrinsic feature space by nonlinear method. In the intrinsic feature space, point A is closer to point B compared to point B under the Euclidean distance. Thus, points A and B can be classified into the same class, whereas point C is classified into another. In contrast, PCA cannot discover the correct relationship among the three points, as shown in Fig. 4(b).

In this paper, we use a typical manifold learning method which is called Isometric mapping (Isomap) [24] to find the low dimension manifold of the data after SWD processing. Isomap seeks to preserve the shortest path along the manifold between any two points x_i and x_j when data are mapped into a low-dimensional subspace. The shortest path can be presented via the geodesic distance $d_G(x_i, x_j)$. To achieve this goal, the process of Isomap is composed by the following steps:

- Step 1: Build the neighborhood graph. Neighborhoods for each point on the manifold are determined based on the Euclidean distances $d(x_i, x_j)$ between pairs of points (x_i, x_j) by a proper method. Generally, there are two methods to determine the neighborhoods. One is to choose k nearest neighboring points, the other is to select all objects within some fixed radius ε. These neighborhood relations are denoted as a weighted graph G over the data set, with edges of weight $d(x_i, x_j)$ between neighboring points.
- Step 2: Estimate the geodesic distances $d_G(x_i, x_j)$ between all pairs of points. $d_G(x_i, x_j)$ can be approximated by the shortest path distances in the graph G:

$$d_G(x_i, x_j) = \begin{cases} d(x_i, x_j) & \text{If } x_i, x_j \text{ are neighborhoods} \\ \min\{d_G(x_i, x_j), d_G(x_i, x_k) + d_G(x_k, x_j)\} & \text{else} \end{cases}$$

  Then we can obtain the shortest path matrix $\mathbf{D}_G = \{d_G(x_i, x_j)\}$.
- Step 3: Find the low-dimensional coordinates. We apply classical Multidimensional Scaling (MDS) [29] to $\mathbf{D}_G$ to build an embedding of the data in a d-dimensional Euclidean space $\mathbf{Y}$ that best preserves the manifold's estimated intrinsic structure. MDS first uses a centering matrix $\mathbf{H} = \mathbf{I} - \frac{1}{n}\mathbf{1}\mathbf{1}^T$ to centralize the geodesic distance matrix $\mathbf{D}_G$, i.e., $\mathbf{B} = -\frac{1}{2}\mathbf{H}\mathbf{D}_G\mathbf{H}$. Here $\mathbf{I}$

is the identity matrix, and $\mathbf{1}$ is a column vector of all one. By performing a spectral decomposition of $\mathbf{B}$, we have $\mathbf{B} = \mathbf{U}\mathbf{\Lambda}\mathbf{U}^T$, where $\mathbf{U}$ is an orthogonal matrix, $\mathbf{\Lambda}$ is a diagonal matrix, and the superscript T means matrix transposition. In order to keep the gram matrix positive semidefinite, the negative elements in the diagonal of matrix $\mathbf{\Lambda}$ are set to 0. Finally, the data $\mathbf{X}$ are reduced to a d-dimensional subspace using an orthogonal matrix $\mathbf{U}_d$ corresponding to $\mathbf{\Lambda}_d$, i.e., $\mathbf{Y} = \mathbf{X}\mathbf{U}_d$.

3.3. Detection Procedure

We take the AMUSAR data for example, Fig. 6 shows the flowchart of our landmine detection procedure. AMUSAR system provides surveillance of large areas via a strip-map SAR mechanism. Fig. 5(a) shows the photos of the system which employs two planar Archimedean spiral antennas with cross-circular polarization. The step-frequency system operates at frequencies of 0.5–2.5 GHz. The airship flies at 100 m above the ground when AMUSAR is working. We choose the time-domain back-projection imaging algorithm [30–34] for its simplicity and good adaptation to motion compensation. Fig. 5(b) shows the optical image of the experimental area with landmines. The area has size of 160 m × 280 m. The spatial sampling rates of the SAR

(a) (b)

Figure 5. (a) Photos of the airship-mounted UWB SAR system; (b) Optical image of the area.

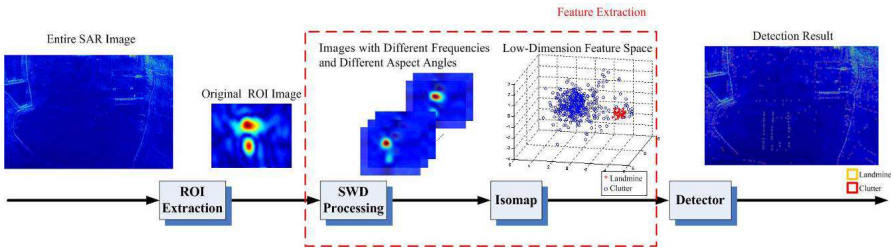

Figure 6. Flowchart of the detection procedure.

image in the ground range direction and azimuth direction are both 0.04 m.

Our landmine detection procedure includes four stages: ROI extraction, SWD processing, Isomap dimension reduction and detection. In the first stage, the CFAR method [35] and morphological filter are used to extract the ROIs. In the second stage, for each ROI, images with different frequencies and different aspect angles are obtained via the SWD processing. In the third stage, low-dimensional feature vectors are formed via the Isomap method. In the last stage, the detection results are obtained via a detector based on the low-dimensional feature vector.

4. EXPERIMENTS RESULTS

The data used in the experiments are also collected by the AMUSAR system. The Signal Noise Ratio (SNR) of the image data is about 14.1 dB. We firstly use the CFAR method and morphological filter to extract the ROIs. The size of each ROI is 21×21 pixels, so the dimensionality of each ROI image is 441. There are aggregately 35 landmines and 500 clutters in the image. Then three feature extraction methods are used to form the feature vectors:

- ***Method A:*** Take 1D range cut through the image center as the feature vector directly. Since the 1D range cut includes 21 pixels, here the dimensionality of feature vector formed by Method A is 21.
- ***Method B:*** Use the PCA method to form the feature vector from the original ROI image.
- ***Method C:*** Proposed Method. We use the SWD processing to obtain images with three different frequencies (1 GHz, 1.5 GHz and 2 GHz) and three different aspect-angles ($-20°$, $0°$ and $20°$). The dimension of the data after SWD processing is 3969 (21×21 pixels $\times$ 3 frequencies $\times$ 3 aspect-angles). Then we use the Isomap to reduce the dimension.

In order to compare the performance of each method on the detection results, the data are randomly divided into two parts: training data and test data, and input a KNN detector after their dimension reduction. The detection is executed six times. Then the average is taken as the result. Fig. 7 illustrates the plots of receiver operating characteristic (ROC) of each method. The dimensionalities of feature vectors formed by each method are all 21. Since the data of range cut through the ROI image center only contain the scattering characteristics in range domain, Method A performs worst.

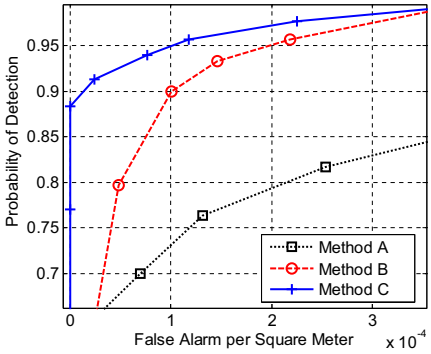

Figure 7. Detection performance of three feature extraction methods (Dim = 21).

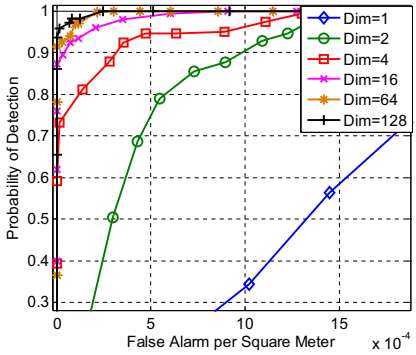

Figure 8. Detection performance of the proposed method with different dimensions.

The scattering characteristics of original ROI image is more abundant than the range cut, so Method B performs better. Finally, Method C performs the best, which contains scattering characteristics in range, azimuth, frequency and aspect-angle domains. Fig. 8 illustrates the plots of ROC of proposed method with different dimensions. The detection performance improves with the dimensionality; however, the improvement becomes small when the dimensionality exceeds 16.

5. DISCUSSION AND CONCLUSION

Extraction of feature vectors with abundant scattering characteristics and low dimension is the key of landmine detection in UWB SAR. In order to construct such feature vectors, the CWD-based SWD processing and Isomap are used in this paper. The former processing is used to obtain the scattering characteristics in four domains: range, azimuth, frequency and aspect-angle. And the latter processing is used to reduce the dimension. The performance of real data processing shows the validity of the proposed method. Knowing that there are other manifold learning methods besides Isomap, for future work, we intend to try other manifold learning methods and develop to detect other types of targets, such as foliage-concealed vehicles.

ACKNOWLEDGMENT

This work was supported by the National Natural Science Foundation of China under Grants 61271441 and 60972121, the Foundation for the

Author of National Excellent Doctoral Dissertation of China under Grant 201046, the Program for New Century Excellent Talents in University under Grant NCET-10-0895 and the research project of NUDT under Grand CJ12-04-02.

REFERENCES

1. Andrieu, J., F. Gallais, V. Mallepeyre, V. Bertrand, B. Beillard, and B. Jecko, "Land mine detection with an ultra-wideband SAR system," *Proceedings of SPIE*, Vol. 4742, 237–247, 2002.
2. Carin, L., N. Geng, M. McClure, J. Sichina, and L. H. Nguyen, "Ultra-wideband synthetic-aperture radar for mine-field detection," *IEEE Antennas Propag. Mag.*, Vol. 41, 18–33, 1999.
3. Wang, Y., Q. Song, T. Jin, X.-T. Huang, and H. Zhang, "A novel minefield detection approach based on morphological diversity," *Progress In Electromagnetics Research*, Vol. 136, 239–253, 2013.
4. Massa, A., A. Boni, and M. Donelli, "A classification approach based on SVM for electromagnetic subsurface sensing," *IEEE Trans. on Geosci. Remote Sens.*, Vol. 43, 2048–2093, 2005.
5. Potin, D., P. Vanheeghe, E. Duflos, and M. Davy, "An abrupt change detection algorithm for buried landmines localization," *IEEE Trans. on Geosci. Remote Sens.*, Vol. 44, 260–272, 2006.
6. Tan, C. P., J. Y. Koay, K. S. Lim, and H. T. Ewe, "Classsification of multi-temporal SAR images for rice crops using combined entropy decomposition and support vector machine technique," *Progress In Electromagnetics Research*, Vol. 71, 19–39, 2007.
7. Sun, Y. and J. Li, "Adaptive learning approach to landmine detection," *IEEE Trans. on Aerosp. Electron. Syst.*, Vol. 41, 973–985, 2005.
8. Halloran, O., B. McGinley, R. C. Conceicao, F. Morgan, E. Jones, and M. Glavin, "Spiking neural networks for breast cancer classification in a dielectrically heterogeneous breast," *Progress In Electromagnetics Research*, Vol. 113, 413–428, 2011.
9. Jin, T. and Z. Zhou, "Feature extraction and discriminator design for landmine detection on double-hump signature in ultrawideband SAR," *IEEE Trans. on Geosci. Remote Sens.*, Vol. 46, 3783–3791, 2008.
10. Casey, K. F. and G. N. Oetzel, "Physical-optics models for scattering from bured mines," *Second Australian-American Joint Conference on the Technology of Mine Countermeasures*, Sydney, Australia, 2001.

11. Cosgrove, R. B., P. Milanfar, and J. Kositsky, "Trained detection of buried mines in SAR images via the deflection-optimal criterion," *IEEE Trans. on Geosci. Remote Sens.*, Vol. 42, 2569–2575, 2004.
12. Wang, T., J. M. Keller, P. D. Gader, and O. Sjahputera, "Frequency subband processing and feature analysis of forward-looking ground-penetrating radar signals for land-mine detection," *IEEE Trans. on Geosci. Remote Sens.*, Vol. 45, 718–729, 2007.
13. Sun, Y. and J. Li, "Plastic landmine detection using time-frequency analysis for forward-looking ground penetrating radar," *Proceedings of SPIE*, Vol. 5089, 851–862, 2005.
14. Savelyev, T. G., L. Kempen, and H. Sahli, "GPR anti-personnel mine detection: Improved deconvolution and time-frequency feature extraction," *Proceedings of SPIE*, Vol. 5046, 232–241, 2003.
15. Wang, Y., Q. Song, T. Jin, Y. Shi, and X. Huang, "Sparse time-frequency representation based feature extraction method for landmine discrimination," *Progress In Electromagnetics Research*, Vol. 133, 459–475, 2013.
16. Jolliffe, I. T, *Principal Component Analysis*, Springer, 1986.
17. Zhang, Y. D., L. N. Wu, and G. W, "A new classifier for polarimetric SAR images," *Progress In Electromagnetics Research*, Vol. 94, 83–104, 2009.
18. Zhang, Y. and L. Wu, "An MR brain images classifier via principal component analysis and kernel support vector machine," *Progress In Electromagnetics Research*, Vol. 130, 369–388, 2012.
19. Martinez, A. M. and A. C. Kak, "PCA versus LDA," *IEEE Transactions on Pattern Analysis and Machine Interlligence*, Vol. 23, 228–233, 2001.
20. Vu, V. T., T. K. Sjören, M. I. Pettersson, L. Hånsson, A. Gustavsson, and L. M. H. Ulander, "RFI suppression in ultrawideband sar using an adaptive line enhancer," *IEEE Geoscience and Remote Sensing Letters*, Vol. 7, 694–698, 2010.
21. Xing, M., X. Jiang, R. Wu, F. Zhou, and Z. Bao, "Motion compensation for UAV SAR based on raw radar data," *IEEE Trans. on Geosci. Remote Sens.*, Vol. 47, 2870–2883, 2009.
22. Zhang, W., F. Liu, L. Jiao, B. Hou, S. Wang, and R. Shang, "SAR image despeckling using edge detection and feature clustering in bandelet domain," *IEEE Geoscience and Remote Sensing Letters*, Vol. 7, 131–135, 2010.
23. Seung, H. S. and D. D. Lee, "The manifold ways of perception,"

Science, Vol. 290, 2268–2269, 2000.

24. Tenenbaum, J. B., V. D. Silva, and J. C. Lanford, "A global geometric framework for nonlinear dimensionality reduction," *Science*, Vol. 290, 2319–2323, 2000.
25. Song, Q., H. Zhang, F. Liang, Y. Li, and Z. Zhou, "Results from an airship-mounted ultra-wideband synthetic aperture radar for penetrating surveillance," *2011 3rd International Asia-Pacific Conference on Synthetic Aperture Radar (APSAR)*, 1–4, Seoul, Korea, 2011.
26. Wong, D. and L. Carin, "Analysis and processing of ultra wide-band SAR imagery for buried landmine detection," *IEEE Transations on Antennas and Propagation*, Vol. 46, 1747–1748, 1998.
27. Krishnapuram, J. S. B. and L. Carin, "Physics-based detection of targets in SAR imagery using support vector machines," *IEEE Sensors J.*, Vol. 3, 147–157, 2003.
28. Jin, T. and Z. Zhou, "Ultrawideband synthetic aperture radar landmine detection," *IEEE Trans. on Geosci. Remote Sens.*, Vol. 45, 3561–3573, 2007.
29. Cox, T. F. and M. A. A. Cox, *Multidimensional Scaling*, Chapman & Hall, London, 1994.
30. Yang, J., X. Huang, T. Jin, J. Thompson, and Z. Zhou, "Synthetic aperture radar imaging using stepped frequency waveform," *IEEE Trans. on Geosci. Remote Sens.*, Vol. 50, 2026–2036, 2012.
31. Jin, T. and Z. Zhou, "Refraction and dispersion effects compensation for UWB SAR subsurface object imaging," *IEEE Trans. on Geosci. Remote Sens.*, Vol. 45, 4059–4066, 2007.
32. Capozzoli, A., C. Curcio, and A. Liseno, "Fast GPU-based interpolation for SAR backprojection," *Progress In Electromagnetics Research*, Vol. 133, 259–283, 2013.
33. Peng, X., W. Tan, Y. Wang, W. Hong, and Y. Wu, "Convolution back-projection imaging algorithm for downward-looking sparse linear array three dimensional synthetic aperture radar," *Progress In Electromagnetics Research*, Vol. 129, 287–313, 2012.
34. Demirci, S., H. Cetinkaya, E. Yigit, C. Ozdemir, and A. A. Vertiy, "A study on millimeter-wave imaging of concealed objects: Application using back-projection algorithm," *Progress In Electromagnetics Research*, Vol. 128, 457–477, 2012.
35. Habib, M. A., "Ca-CFAR detection performance of radar targets embedded in 'non centered chi-2 Gamma' clutter," *Progress In Electromagnetics Research*, Vol. 77, 135–148, 2008.